Time resolved build-up and decay of photorefractive and free carrier gratings in CdTe:V

Kestutis Jarašiunas, Philippe Delaye, Gérald Roosen, Jean-Claude Launay

F-VIII.3

TIME RESOLVED BUILD-UP AND DECAY OF PHOTOREFRACTIVE AND FREE CARRIER GRATINGS IN CdTe:V

Kestutis Jarasiunas[1*] , Philippe Delaye[1], Jean-Claude Launay[2], Gérald Roosen[1]

1) Institut d'Optique Théorique et Appliquée, Unité de Recherche Associée 14 au Centre National de la Recherche Scientifique, Centre Scientifique d'Orsay, B.P.147, 91403 Orsay Cedex, France, Tel: (1)69416855, Fax: (1) 69413192.

2) Pôle de Recherche Aquitain pour les matériaux dans l'espace (Prame), B.P.11, 33165 Saint Médard en Jalles Cedex, France

Abstract. Laser induced picosecond transient gratings are used to study carrier transport via free carrier and photorefractive nonlinearities. Feed-back effect of light induced space charge electric field is found responsible for diffracted beam intensity oscillations during the grating recording and its decay.

Introduction. Photorefractive semiconductor crystals are of great interest for high speed optical processing in near infrared. Optical nonlinearities of different origins and various refractive index modulation mechanisms take place in these crystals under excitation by short powerful laser pulses at 1.06 μm [1-7]. We present time resolved and excitation energy dependent analysis of carrier transport and of space charge field mechanisms in photorefractive CdTe:V. This kind of studies may help to optimize crystal parameters for different applications as well as to improve nonlinear optical techniques for determining electrical parameters of semiconductors.

Experimental set-up. Carrier transport studies in vanadium doped CdTe were performed by using degenerate 4-wave mixing technique at 1.06 μm (Fig.1). A YAG laser with pulse duration τ_L = 28 ps FWHM and output energy up to 10 mJ.cm^{-2} was used. Two s-polarized beams of equal intensities were used for recording a grating with period Λ = 1.8 μm. The semi-insulating crystal (ρ =5.10^8 Ω.cm) was grown by using the modified Bridgman technique and vanadium doped to 10^{19} cm^{-3} to produce deep donor level at ≈E_C-0.75 eV [8]. The absorption coefficient of the d= 5 mm thick sample is measured equal to 2 cm^{-1} at λ=1.06 μm. The sample was cut with faces along crystallographic directions (110), (-110), and (001). In our experiments the orientation of the grating vector *Kg* was along (110) or (001) directions. Probe and diffracted beam polarization states were monitored to separate coexisting refractive index gratings from different origins. The cases when pure photorefractive (PR) grating (i.e. p-diffracted component of s-polarized probe beam for *Kg* along (110)) or pure free carrier (FC)

---

* Material Research Laboratory *INTEST,* Semiconductor Physics Department of Vilnius University, Sauletekio 9, bld.3, Vilnius 2054, Lithuania

grating (p-diffracted component of p-polarized probe beam for *Kg* along (110) or (001)) have been analyzed experimentally. A Glan-polarizer oriented to reflect p-polarization was used for separation of Bragg-diffracted beam counterpropagating to one of the recording beams. The separated beam was directed to a fast silicon photodiode through the next p-transmitting polarizer. Such a set-up allows us to detect diffracted signals as low as 10^{-6}-10^{-7}. Diffracted beam intensity $\langle I_1 \rangle$ or grating efficiency $\eta = \langle I_1 \rangle / \langle I_T \rangle$ (here $\langle I_1 \rangle$ and $\langle I_T \rangle$ are time-integrated values of diffracted and transmitted probe beams) as a function of excitation level E and of probe beam delay time Δt are studied. For qualitative analysis of processes involved in carrier and space charge field dynamics we solved the set of six material equations [1,5] assuming that carrier generation from and via deep traps dominates.

Results and discussion. In Fig.2 the exposure characteristics (EC) for FC and PR gratings (i.e dependences of the diffracted beam intensity $\langle I_1 \rangle$ versus excitation energy I) are presented. EC of a semiconductor contains the main information about carrier generation It usually follows a power-law dependence at low excitations energies, $\langle I_1 \rangle = I^{\gamma}$ with γ -value corresponding to carrier generation rate [9]. Assuming that carrier concentration ΔN increases with excitation by power law as $\Delta N = I^{\beta}$, we have the following relationship between slopes γ and β in the region of linear transmittance T of the sample (i.e. low excitations)

$$\langle I_1 \rangle = \langle I_T \rangle \ (\pi \Delta n \, d/\lambda)^2 = I\,T\,(\pi n_{eh} \Delta N d/\lambda)^2 = A I^{2\beta+1} = A I^{\gamma} \qquad (1)$$

here $\Delta n = n_{eh} \Delta N$ is the refractive index modulation of the grating, with ΔN the spatially modulated free carrier concentration and n_{eh} is the refractive index change due to one electron hole pair.

In a general case, band- to-band linear carrier generation will lead to value $\beta = 1$ and corresponding $\gamma = 3$; for two photon light absorption process $\beta = 2$ and $\gamma = 5$. In our CdTe:V sample, γ -values reveal three excitation regions corresponding to different light absorption mechanisms. For FC gratings, we observe carrier generation from deep levels altered by two-step transitions via impurity states (γ=4), two-step and two-photon absorption of light (γ =5), and, finally, the saturation of diffracted beam intensity at high excitations. The defocussing of transmitted and diffracted beams at high excitations was observed, and this may be the reason for FC grating profile distorsions leading to $\langle I_1 \rangle$ saturation. To avoid this, we mainly carried out our measurements at $E \leq 5$ mJ.cm^{-2}. Photorefractive nonlinearity, because its lower sensitivity, reveals two-step and two-photon carrier generation (γ =5) at lower excitations with the following decrease of EC slope from value $\gamma = 5$ to $\gamma = 3$ at higher excitations (linear increase with energy). This linear increase of the space charge field with excitation while the carrier concentration increases more rapidely in a nonlinear way points out that space charge field dynamics is more complicated than FC

processes. Indeed, in this regime, both electrons and holes are generated and can compete giving opposite contributions to the space charge field.

Measurements of sample transmittivity vs. excitation energy (Fig.3) have shown a tendency of absorption bleaching at low fluences and revealed the increasing role of nonlinear absorption with energy. In this way, transmittivity measurements confirmed the observed processes of carrier generation .

Carrier transport peculiarities have been observed in the dynamics of both FC and PR gratings.(Fig. 4 and 5) We found that the FC grating decay time τ_g varies with excitation energy and with time. The fastest average grating decay time τ_{g1} = 80-100 ps was observed at the lowest excitations used here (≈1 mJ.cm^{-2}). With increasing the incident power, the decay speed was slowering untill it reached the value $\tau_{g2} \approx 230$ ps. At high excitation energies the decay rate slowers also with time: at $\Delta t \geq 600$ ps we found $\tau_{g3} \approx$ 365-410 ps. FC gratings decay finally with time constant of 1.7 ns which we attributed to carrier recombination time.

The processes of carrier diffusion and drift in light induced space charge (SC) field must be taken into account to explain the observed behaviour. One must consider that the value of created electric field E_{sc} is dependent on carrier redistribution and thus varies with time. Electron diffusion during the action of laser pulse will create a SC field between the mobile charges and ionized deep traps. Then hole related processes may be observed: (i) the hole drift to grating minima will reduce the negative charge in these positions due to the previous diffusion of electrons and (ii) the build-up of a pure hole grating (that is π–shifted from its former position) will take place after the holes will reach the minima of light interference field (here E_{sc} =0). Such a behaviour of free carrier grating was predicted by computer simulation of carrier dynamics in photorefractive crystals [5]. Thus, the role of holes is more and more increasing with time but in addition it increases also with excitation. In a general case, the average speed of FC grating decay will be governed by carrier bipolar diffusion related to electron-hole concentration at the given moment. The value of the bipolar diffusion coefficient D_a are given by eq. (2):

$$D_a = kT\mu_a / e = (kT/e)(\Delta N + \Delta P) / (\Delta N / \mu_h + \Delta P / \mu_e) \qquad (2)$$

with μ_a the bipolar mobility, and ΔN (ΔP) the spatially modulated concentration of free electrons (holes).

Thus the grating decay constant at the lowest excitations τ_{g1} corresponds to μ =330-410 cm^2.V^{-1}.s^{-1} » μ_h, showing that the electron generation is much more efficient than the hole one. At higher excitations decay slowers as hole concentration approaches electron one, and value $\tau_{g2} \approx 230$ ps corresponds to carrier ambipolar mobility for the case $\Delta N = \Delta P$ with the value μ_a =135-140 cm^2.V^{-1}.s^{-1} following from eq.2. The value of hole mobility μ_h = 80-90 cm^2.V^{-1}.s^{-1}, a typical value one for CdTe [10], was obtained from decay time τ_{g3}.

Photorefractive gratings (PR) have shown two decay times at high excitations (Fig.5), when $\eta \geq 5.10^{-6}$. The fast decay has a time constant τ_1 = 220-230 ps that corresponds to an ambipolar carrier diffusion coefficient equal to 3.56-3.73 $cm^2.s^{-1}$. Thus the origin of this refractive index modulation mechanism is a transient Dember field between mobile carriers. At longer delays or at lower excitation levels a slow component of grating decay with $\tau_2 \approx$ 700 ps dominates. We attribute it to the relaxation of the ionic grating created in deep traps. Rough estimation of the SC field relaxation time τ_{SC} was made for these conditions by using formula for the dielectric relaxation time modified by a grating factor [11] and experimental values from FC grating measurements: carrier concentration $N \approx 3.10^{14}$ cm^{-3}, their lifetime τ_R = 1.7 ns and electron mobility μ_e = 520 $cm^2.V^{-1}.s^{-1}$. A good agreement between the calculated value $\tau_{SC} \approx$ 600 ps and the experimental one was found. In fact, the relaxation time is dependent on the ionized donor concentration and will vary in time scale. What we observed is probably the fastest component of τ_{SC} after the Dember field has decayed.

We performed computer simulations of carrier and E_{SC} dynamics for two cases: high excitation case when N=P and low excitation case when N>>P (Fig.6). The fast decay of the grating by electron diffusion creates a SC field which in turn slowers the FC grating decay and prevents its from a total decay. At high excitations ambipolar diffusion governs the grating decay and the Dember field dominates over E_{SC} in deep traps. This kind of PR and FC grating behaviour was found experimentally too.

The simultaneous existence of two refractive index modulation mechanisms and their interaction lead to peculiarities observed in time-resolved grating build-up and decay. We have observed a step-like increase of the diffracted beam intensity during the action of laser pulse as well as saw-like oscillations (i.e. a fine structure of very fast decay and recovery of the grating on an essentially slower slope of diffusive grating decay) (see Fig.4,5). We attribute this to a feed-back effect of the created space-charge field on the grating modulation, i.e. to the redistribution of the electron concentration due to the SC field. In addition to impeding their diffusion, the field will inforce carriers to move back to grating peaks from previous nearly homogeneous distribution. This will lead to electron grating reconstruction and to an increase of the grating efficiency. During the action of laser pulse, the competition of carrier generation, their diffusion and drift may create a continuing process of variation of τ_g which will lead to a step-like shape of the grating build up. A similar shape of grating formation was observed in type-II quantum well heterostructures [12] where carrier confinement to the different layers leads to induced electric field.

This fine structure of grating decay and build-up exists on both FC and PR grating decay curves what shows that grating modulation and E_{SC} temporal value do not equilibrate independently. A time and space varying feed-back strength may create trapezoidal carrier distribution with steep edge at position l= Λ/4. As discussed in [1],

at low excitations the drift current evolves as the square of the input fluence while the diffusion current remains linear. The modelisation of carrier dynamics in nonhomogeneous electric fields is a very complicated task indeed. The linear modelisation we have given above has not shown evidences of temporal oscillations. However, experiments of light diffraction on FC gratings in external strong microwave fields [13] (with electric vector oriented along the grating vector as in our experiments) have also shown similar peculiarities of diffracted signal: an increase of diffraction efficiency that was dependent on grating period and five-fold stronger in GaAs than in Si, i.e. related to electron mobilities.

Further analysis of the obtained data allows us to calculate the electron mobility in CdTe:V. Using the average value of hole mobility $\mu_h = 85$ cm^2.V^{-1}.s^{-1} (from FC decay) and the ambipolar one, $\mu_a = 146$ cm^2.V^{-1}.s^{-1} (obtained from Dember field decay of PR grating, i.e. for the case $\Delta N = \Delta P$), we calculate $\mu_e = 520$ cm^2.V^{-1}.s^{-1}. This value is twice smaller than in undoped CdTe [10]. The reason is probably a more efficient carrier scattering by neutral and ionized impurities. The mobility-lifetime product $\mu_e\tau_R = 8.8\ 10^{-7}$ cm^2.V^{-1} follows from our measurements and is in good agreement with the one obtained for electrons by CW photorefractive gain measurements in this crystal ($\mu\tau = 8.10^{-7}$ cm^2.V^{-1} [8]). In addition, this transient grating technique permits detail studies of electron and hole generation rates. Directly measured grating decay times will give values of μ_a and thus the corresponding N/P ratios at different excitation fluences will be obtained.

Conclusion. We have demonstrated that the simultaneous investigations of coexisting optical nonlinearities in photorefractive media allow direct studies of crystal properties as monopolar carrier mobilities and carrier concentrations. This kind of knowledge is very important for the understanding of deep level behaviour with excitation energy, wavelength, doping, etc... Diffracted beam intensity oscillations during grating build-up and its decay were found and explained qualitatively by light induced space-charge field feed-back effect on carrier transport .

Acknowledgment. K.Jarasiunas acknowledges the support by M.R.T-France.

REFERENCES

[1] A.L.Smirl, G.C.Valley, K.M.Bohnert, and T.F.Boggess, IEEE J. Quantum Electron. QE-24 (1988) 289 .

[2] M.S.Petrovic, A.Suchocki, and R.C.Powell, J. Appl. Phys. 66 (1989) 1359.

[3] W.A.Shroeder, T.S.Stark, T.F.Boggess, A.L.Smirl, and G.C.Valley, Opt. Lett. 16 (1991) 799.

[4] W.A.Shroeder, T.S.Stark, M.D.Dawson, T.F.Boggess, A.L.Smirl, and G.C.Valley, Opt. Lett. 16 (1991) 159.

[5] L. Disdier and G.Roosen, Optics Comm. 88 (1992) 559.

[6] J.Vaitkus, E.Gaubas, K.Jarasiunas, and M.Petrauskas, Semicon. Sci. Technol. 7 (1992) A131.

[7]K. Jarasiunas, Ph.Delaye, J.C. Launay,and G.Roosen, Opt. Commun., (1992), in press.

[8] J.C. Launay, V.Mazoyer, M.Tapiero, J.P.Zielinger, Z.Guellil, Ph.Delaye, and G.Roosen, Appl. Phys. A 54 (1992), in press.

[9] J.Vaitkus, K.Jarasiunas, E.Gaubas, L.Jonikas, R.Pranaitis, and L.Subacius, IEEE J. Quantum Electron. QE-22 (1986) 1298.

[10] A.J.Strauss, Rev. Phys. Appl. 12 (1977) 167.

[11] J.P.Huignard and G.Roosen, in: Nonlinear Optics: Materials and Devices, eds. C.Flytzanis and J.L.Oudar (Springer-Verlag, Berlin Heidelberg,1986) p.128.

[12] H.Weinert, K.Jarasiunas, and B.Shumann, Phys. Stat. Sol. (a) 114 (1989) K183.

[13] J.Vaitkus, E.Starikovas, L.Subacius, and K.Jarasiunas, Lietuvos Fizikos Rinkinys, 30, (1990) 336 (in Russian; transl. to English in Sov.Phys.- Collections, Allerton Press Inc. N.Y., USA.

FIGURE CAPTIONS

Fig.1. Experimental set-up: GP - Glan polarizer, λ/2 - half-wavelength plate, D - detector.

Fig.2. Dependence of diffracted probe beam intensity $\langle I_1 \rangle$ and efficiency η vs. recording energy I for free carrier (FC) and photorefractive (PR) gratings (probe beam delay time corresponds to the end of the laser pulse; sample orientation Kg along (110)).

Fig.3. Transmittivity of the sample at different excitation energies for p-polarized probe beam (filled circles) and for s-polarized one (open circles).

Fig.4. Free carrier (FC) grating dynamics at high excitation energies: E = 8.5 ± 0.5 $mJ.cm^{-2}$ (1), 6.5 ± 0.3 $mJ.cm^{-2}$ (2), 4.5 ± 0.25 $mJ.cm^{-2}$ (3), and 3.75± 0.25 $mJ.cm^{-2}$ (4); sample orientation, Kg along (110).

Fig.5. Photorefractive (PR) grating build-up and decay at different excitation levels:

E= 6.5 ± 0.5 $mJ.cm^{-2}$ (1), 4.75 ± 0.25 $mJ.cm^{-2}$ (2), 2.88 ± 0.12 $mJ.cm^{-2}$ (3), and 1.88 ± 0.12 $mJ.cm^{-2}$ (4); sample orientation, Kg along (110). Error bars are presented on curve 2 showing the reality of the oscillations.

Fig.6. Computer simulations of carrier and space charge field dynamics for two cases: low excitation case (N>>P, on left side) and high excitation case (N=P, right side). Abbreviations correspond to refractive index modulation (Δn), electric space sharge field (E_{sc}), electron and hole grating modulation depths (N_1 and P_1); here $\Delta n = N_1/m_e + P_1/m_h$ .We used the following parameters for calculations: deep trap density - 4.10^{16} cm^{-3}, ionization cross-sections for electrons and holes $S_n = S_p = 5.10^{-17}$ cm^2 , carrier recombination coefficients $\gamma_n = 10\gamma_p = 1.2\ 10^{-7} cm^3.\ s^{-1}$, μ_e = 520 $cm^2.V^{-1}.s^{-1}$, μ_h = 80 $cm^2.V^{-1}.s^{-1}$. Note: the delay in E_{sc} build-up at low excitations is an important feature pointing out diffusive origin of E_{sc}. This was observed experimentally only at low excitations (Fig.5).

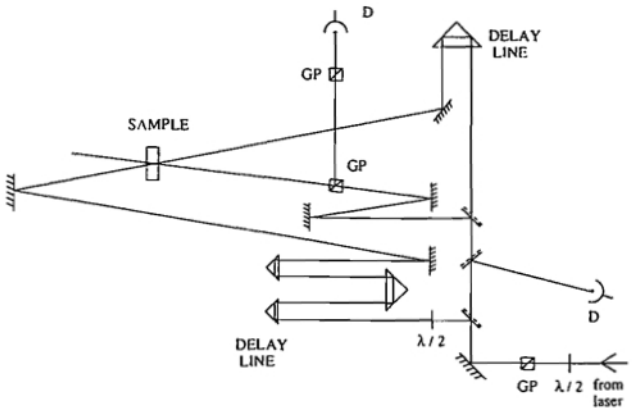

Figure 1

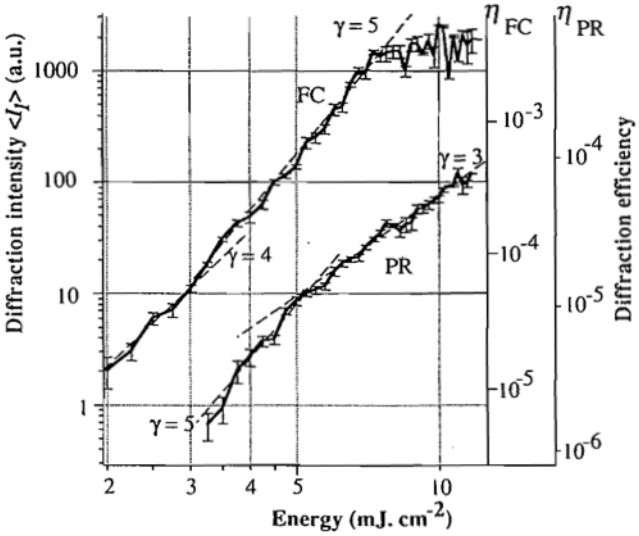

Figure 2

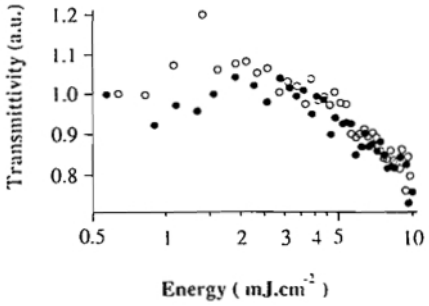

Figure 3

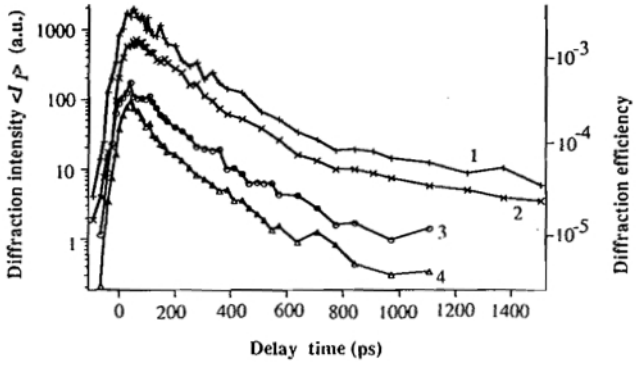

Figure 4

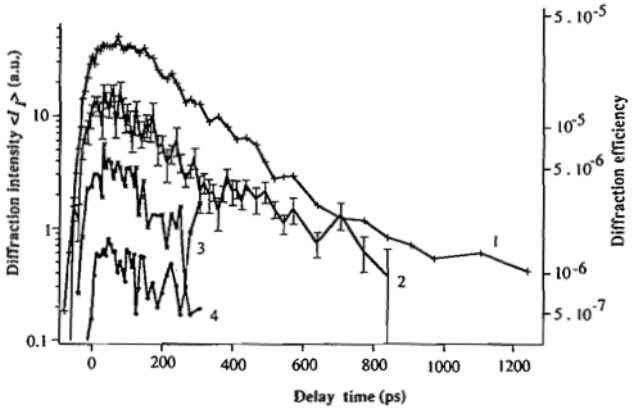

Figure 5

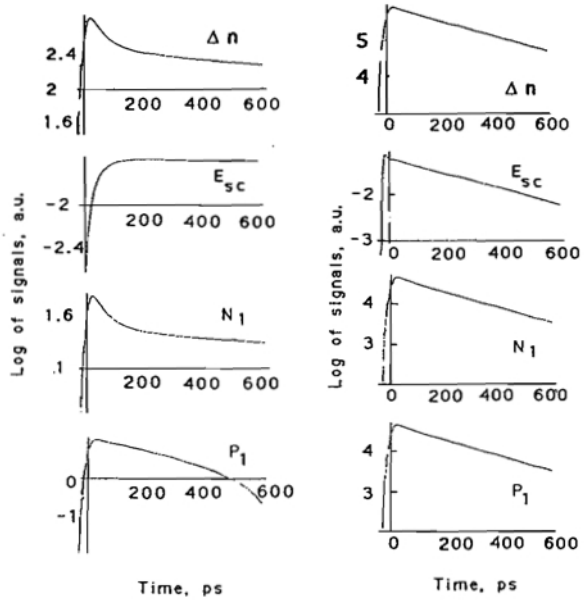

N>>P **N=P**

Figure 6